Chinese Journal of Chemistry
中国化学 - An International Journal

Check for updates

Accepted Article

Title: Near-infrared fluorescent nanoprobe for detecting hydrogen peroxide in inflammation and ischemic kidney injury

Authors: Lingfeng Xu, Lihe Sun, Fang Zeng,* and Shuizhu Wu*

This manuscript has been accepted and appears as an Accepted Article online.

This work may now be cited as: *Chin. J. Chem.* **2020**, *38,* 10.1002/cjoc.202000166.

The final Version of Record (VoR) of it with formal page numbers will soon be published online in Early View: http://dx.doi.org/10.1002/cjoc.202000166.

WILEY-VCH SIOC CCS

ISSN 1001-604X • CN 31-1547/O6
mc.manuscriptcentral.com/cjoc
www.cjc.wiley-vch.de

Near-infrared fluorescent nanoprobe for detecting hydrogen peroxide in inflammation and ischemic kidney injury

Lingfeng Xu,[a] Lihe Sun,[a] Fang Zeng,*[,a] and Shuizhu Wu*[,a]

[a] *State Key Laboratory of Luminescent Materials & Devices, Guangdong Provincial Key Laboratory of Luminescence from Molecular Aggregates, College of Materials Science & Engineering, South China University of Technology, Guangzhou 510640, China*

Cite this paper: *Chin. J. Chem.* **2019**, *37*, XXX—XXX. **DOI: 10.1002/cjoc.201900XXX**

Summary of main observation and conclusion In-situ overexpressed hydrogen peroxide could serve as a biomarker for inflammation and ischemic kidney injury. Herein a nanoprobe was developed for assaying of hydrogen peroxide. The nanoprobe (TA-TPABQ) was formed *via* the boronate ester groups between the hydrophilic tannic acid and the boric-acid-containing compound (TPABQ) as well as the hydrophobic interactions. The probe with good photostability shows good sensitivity and selectivity towards H_2O_2. The probe was adopted for identifying endogenous and exogenous H_2O_2 in living cells. Moreover, the probe was utilized for *in vivo* imaging experiments in acute abdomina and ankle inflammation mouse models as well as acute renal ischemia mouse model.

Background and Originality Content

As redox homeostasis is crucial for various cellular functions, many disordered physiological processes are usually associated with the abnormal level of oxidative stress (elevated intracellular level of reactive oxygen species (hereinafter referred to as ROS).[1-4] H_2O_2 is one of the important members of ROS and is overexpressed in a variety of diseases,[5-8] including the acute abdominal inflammation[9] and renal ischemia injury.[10] Thus, the in-situ hydrogen peroxide level in the foci of these diseases could serve as a biomarker for them, and therefore the sensitive in-situ detection for H_2O_2 level in the diseases' site is of great importance in terms of possible early diagnosis for these diseases.[8-10]

Fluorescence detection technique is one of the effective and convenient imaging tools to identify the target biomarkers in bio-system.[11-20] Compared to other methods, fluorescence technique shows higher sensitivity, simple operation process and non-destructive imaging capability.[21-24] To date, various fluorescent probes especially those with long-wavelength emission have been synthesized for H_2O_2 detection, as summarized in Table S1. However, most of the reported probes display short Stokes shift, and are hydrophobic and tend to aggregate in aqueous biological system, their fluorescence may be quenched due to the π-π stacking and thus be deleterious for fluorescence response.[25-27] Nevertheless, the fluorophores with aggregation-induced emission (AIE) can readily avoid the aggregation-caused quenching, this feature is beneficial for fluorescence imaging in bio-system.[28-39] However, only a few organic probes have been developed for H_2O_2 detection with AIE characteristic, and most of them still suffered from short wavelength emission (< 650 nm).[40-44]

In order to construct an activatable near-infrared nanoprobe for detecting H_2O_2 overexpression in diseases, herein we developed the TA-TPABQ nanoprobe, as shown in Figure 1. The hydrophobic compound TPABQ forms the boronate ester bonds (dynamic-covalent bonding linkage)[45-47] with the hydrophilic natural polyphenol tannic acid (TA), and then the nanoparticle (nanoprobe) readily forms owing to the boronate ester bonds and the hydrophobic interactions. The boronate ester bonds can serve as the recognition moiety for H_2O_2, as hydrogen peroxide can readily cleave boronate ester.[48-50] In the absence of H_2O_2, the fluorescence intensity of the probe was very weak at 725 nm, whereas strong fluorescence signals occurred when the probe was exposed to H_2O_2. Upon the probe's reaction with H_2O_2, the activated probe namely the resultant product (theoretically the product is TPAQ-OH) exhibited remarkable fluorescence in the aggregated state because of its hydrophobicity and AIE feature. The probe was adopted for identifying endogenous and exogenous H_2O_2 in living cells (RAW264.7, HepG2 and HeLa). Moreover, the probe was utilized for *in vivo* imaging experiments in acute abdomina and ankle inflammation mouse models as well as acute renal ischemia mouse model.

Results and Discussion

Synthesis and spectral properties of the nanoprobe TA-TPABQ

The compound TPABQ was synthesized according to Scheme S1. Then the nanoprobe TA-TPABQ was obtained with TPABQ and tannic acid (TA) through the boronate ester bonds and hydrophobic interaction. Moreover, the TPAQ-OH (theoretical product of the reaction between the nanoprobe TA-TPABQ and H_2O_2) was synthesized as well, as shown in Scheme S2. The intermediate products and TPAQ-OH were characterized by 1H NMR and MS

spectrometry (Figure S1-Figure S8). The final nanoprobe TA-TPABQ was investigated by X-ray photoelectron spectroscopy (XPS) as well (Figure S9). The particle size of TA-TPABQ was approximately 100 nm, and that of the TPAQ-OH aggregates was around 120 nm based on the dynamic light scattering (DLS) method (Figure S10). The content of TPABQ in the nanoprobe was determined as 29.7 wt%, through the absorption spectrometry by referring to the predetermined calibration curve.[51] As shown in Figure 1b and Figure 1c, in the absence of H_2O_2 the nanoprobe TA-TPABQ showed only weak fluorescence at 725 nm; whereas strong fluorescence appeared at around 725 nm in the presence of H_2O_2. The electron-withdrawing boronate ester groups quench the fluorescence of TPABQ; while when hydrogen peroxide reacts with the nanoprobe, the boronate ester bonds are cleaved, and the electron-donating hydroxyl group is generated on the fluorophore TPAQ-OH, thus the fluorescence is restored. As for the absorption spectra, the nanoprobe TA-TPABQ displayed the maximal absorption at 527 nm in the absence of H_2O_2. These data indicate that the nanoprobe TA-TPABQ is suitable to serve as a turn-on reporter for H_2O_2.

The AIE feature of TPAQ-OH (the theoretical product from the reaction between TA-TPABQ and H_2O_2) in the good solvent of THF and the poor solvent PBS mixture was investigated according to the reported method.[52,53] The fluorescence spectra were obtained in the PBS/THF mixture with various PBS volume fractions (f_p) ranging from 0%-90%. As displayed in Figure 2a and Figure 2b, there was negligible emission when f_p was below 30%, and fluorescence intensities gradually increased with the increasing fraction of PBS. Especially, when f_p reached 90%, the fluorescence intensity increased dramatically with about 46.7-fold enhancement compared with that in good solvent of THF.

Detection mechanism and fluorescent response of the nanoprobe TA-TPABQ towards H_2O_2

As boronate ester bonds can be cleaved by H_2O_2,[3] upon the nanoprobe TA-TPABQ being reacted with H_2O_2, the fluorophore TPAQ-OH is generated, and thus the TPAQ-OH molecules aggregate and give out strong fluorescence. To confirm the detection mechanism, the absorption and emission spectra for the nanoprobe TA-TPABQ upon being reacted with H_2O_2 and those of the synthesized TPAQ-OH (theoretical reaction product) were compared (Figure S11 and Figure S12). It could be observed that the absorption and emission spectra of the product after the nanoprobe being reacted with H_2O_2 were quite similar to those of the synthesized theoretical reaction product TPAQ-OH. Furthermore, the ^1H NMR spectrum of the reaction product obtained from the reaction between the nanoprobe and H_2O_2 and that of the synthesized theoretical reaction product TPAQ-OH were found to be similar (Figure S13). These results confirm that TPAQ-OH is indeed generated after the reaction between the TA-TPABQ and H_2O_2. Moreover, a large Stokes shift (198 nm) was found in the resultant product TPAQ-OH, as shown in Figure S14. This feature is beneficial for bio-detection and imaging, since large Stokes shift can avoid the interfaces of molecular self-absorption effectively.

Next, the fluorescence response of the nanoprobe TA-TPABQ towards H_2O_2 as function of incubation time is shown in Figure 2c and Figure 2d. Obviously, the fluorescence intensity increased with the extended incubation time, and reached a plateau within 15 min. Also, as shown in Figure 2e and Figure 2f, the fluorescence intensity increased gradually with the increasing concentration of H_2O_2. A linear correlation between the fluorescence intensities (at 725 nm) and H_2O_2 concentrations in the range of 0-40 μM was obtained, and the limit of detection (LOD) was calculated to be 117 nM (Figure S15).

Then the selectivity of the nanoprobe TA-TPABQ for H_2O_2 detection was tested; various anionic ions, cationic ions and bio-molecules were incubated with the nanoprobe TA-TPABQ, and the fluorescence intensities were recorded as displayed in Figure S16. The various substances showed negligible fluorescent changes compared with the control group (the nanoprobe TA-TPABQ solution). Whereas, significant fluorescence enhancement was observed after the nanoprobe's incubation with H_2O_2. Moreover, several kinds of reactive oxygen species ($ONOO^-$, ClO^-, H_2O_2, *etc.*) and nitrogen species (NO_3^-, NO_2^-, NO) were incubated with the TA-TPABQ as well, and negligible fluorescence enhancement was induced under the same conditions. The results show that the nanoprobe TA-TPABQ possesses high selectivity toward H_2O_2, and the fluorescence signal won't be interfered by these substances, hence the nanoprobe may be suitable for application in complex biological system. Also, the fluorescence intensities were measured in the solutions under various pH values (6.5-8.0). As presented in Figure S17, the fluorescence intensity of the TA-TPABQ remained relatively stable in the physiological pH range. In the meantime, for the TA-TPABQ, with the treatment of H_2O_2 in the same pH range, an obvious enhancement of fluorescence signal occurred, and the corresponding fluorescence intensity varied slightly in this pH range. In addition, the photo-stability of the nanoprobe TA-TPABQ was investigated under the continuous irradiation by the xenon lamp with or without the existence of H_2O_2. As displayed in Figure S18, the fluorescence intensity in the time range of 0-120 min were measured, and results showed that the nanoprobe TA-TPABQ and the reaction product displayed good photo-stability. The nanoprobe TA-TPABQ exhibited high stability after 4 days' incubation in saline, as confirmed by DLS results (as shown in Figure S19). The good stability of the nanoprobe indicates that it is suitable for imaging in biological system.

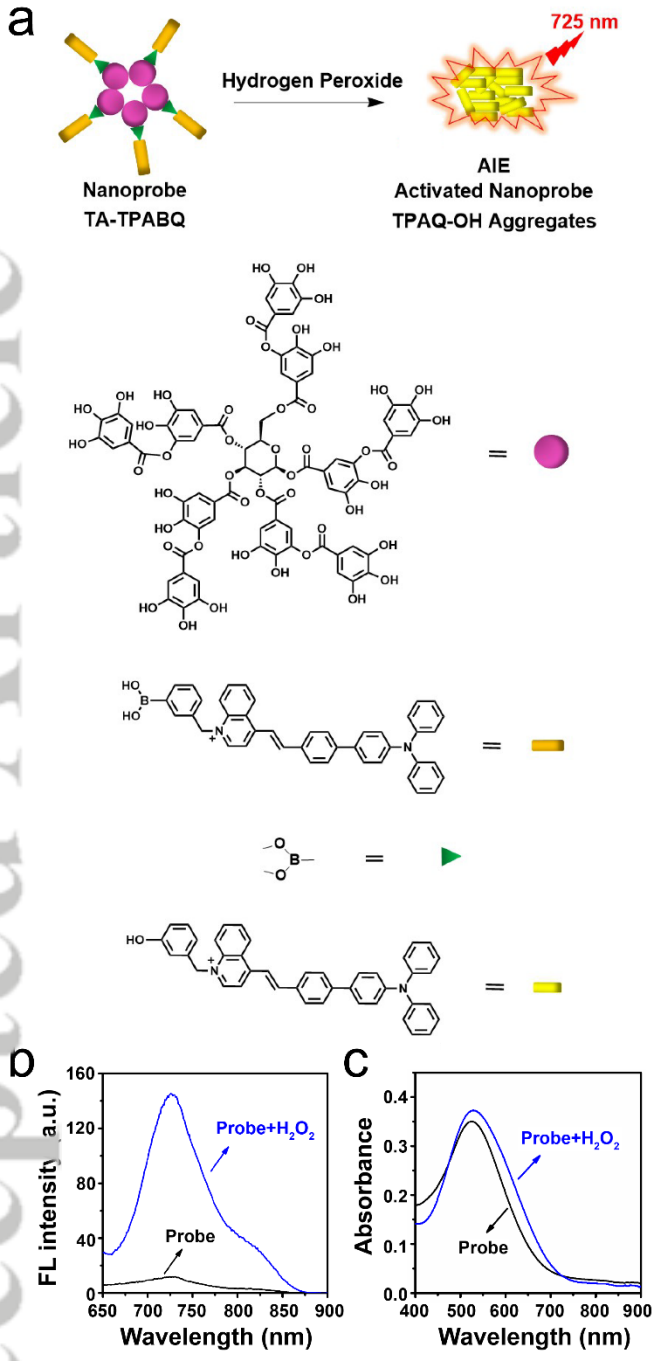

Figure 1 (a) Schematic illustration of the nanoprobe TA-TPABQ for H_2O_2 detection. (b) Fluoescence spectra of the nanoprobe TA-TPABQ (TPABQ 10 μM) before or after the incubation of H_2O_2 (60 μM) in PBS (10 mM, pH 7.4). (c) Absorption spectra of the nanoprobe TA-TPABQ (TPABQ 10 μM) before or after the incubation of H_2O_2 (60 μM) in PBS (10 mM, pH 7.4).

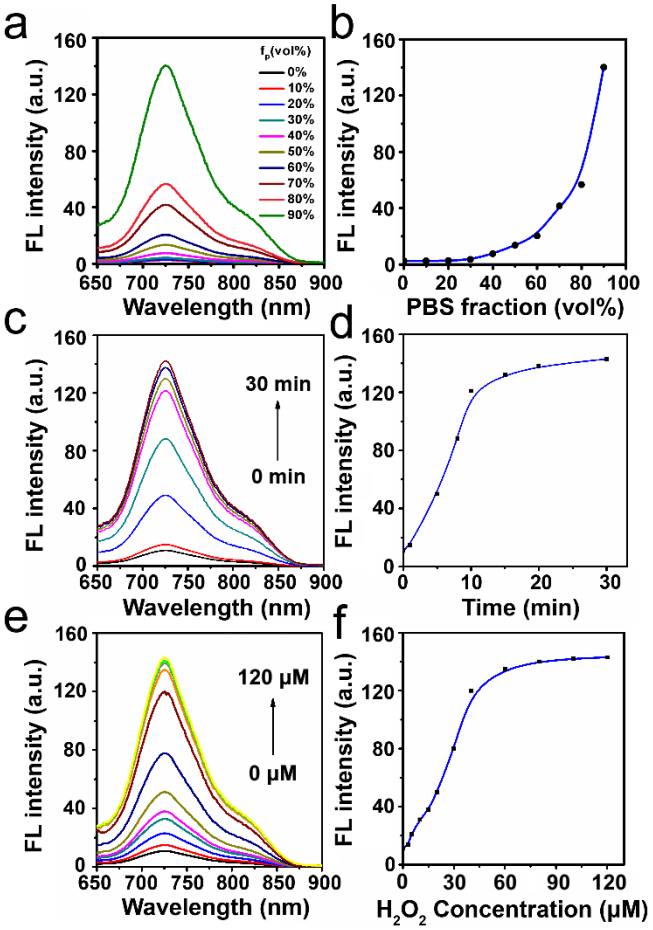

Figure 2 (a) Fluorescence spectra of TPAQ-OH (10 μM) in PBS/THF mixture with different PBS volume ratios (from 0%-90%), λ_{ex} = 580 nm. (b) Fluorecence intensity at 725 nm of TPAQ-OH (10 μM) in PBS/THF mixture with different PBS volume ratios (from 0%-90%). (c) Fluorescence spectra of the nanoprobe TA-TPABQ (TPABQ 10 μM) exposed to the H_2O_2 (60 μM) for different incubation time (0-30 min) in PBS (10 mM, pH 7.4). (d) Fluorescence intensities at 725 nm of the nanoprobe TA-TPABQ (TPABQ 10 μM) after being exposed to the H_2O_2 (60 μM) for different incubation time (0-30 min) in PBS (10 mM, pH 7.4). (e) Fluorescence spectra the nanoprobe TA-TPABQ (TPABQ 10 μM) upon incubation with various concentrations of H_2O_2 (0-120 μM) for 30 min in PBS (10 mM, pH 7.4). (f) Fluorescence intensities at 725 nm of the TA-TPABQ (TPABQ 10 μM) after being reacted with various concentrations of H_2O_2 (0-120 μM) for 30 min in PBS (10 mM, pH 7.4).

Fluorescence imaging of H_2O_2 in living cells

The nanoprobe's capability of detecting H_2O_2 in living cells was evaluated. Prior to the imaging experiments, the cytotoxicities of the nanoprobe TA-TPABQ against the RAW264.7 (mouse monocyte macrophage cell line), HepG2 (human hepatoma cell line), HeLa (human cervical cancer cell line) and L929 (mouse fibroblast cell line) were estimated. As displayed in Figure S20, high cell viabilities

remained after incubation with the TA-TPABQ, even when the nanoprobe's concentration reached 60 μM. The results indicate that the nanoprobe TA-TPABQ presents little cytotoxicity towards these kinds of cell lines. After that, the nanoprobe TA-TPABQ was utilized to image H_2O_2 in RAW264.7, HepG2 and HeLa cell lines. As shown in Figure 3a, Figure S21a and Figure S22a, when the living cells were only treated with the TA-TPABQ, weak fluorescence signals could be observed. Whereas, when phorbol myristate acetate (PMA) was employed as a stimulator to trigger the up-regulation of intracellular H_2O_2,[54] the fluorescence signals increased obviously in the three cell lines. By contrast, it could be found that fluorescence decreased apparently in the presence of N-acetylcysteine (NAC),[55] a widely used antioxidants for H_2O_2 elimination. The results confirm that the nanoprobe TA-TPABQ is capable of detecting endogenous H_2O_2 in these three cell lines. Then the nanoprobe TA-TPABQ was applied to image the exogenous H_2O_2 in these three living cell lines. The exogenous H_2O_2 was added into these three living cells lines during the culturing process, and obvious fluorescence signal could be observed, suggesting that the fluorescence was triggered by the exogenous H_2O_2.

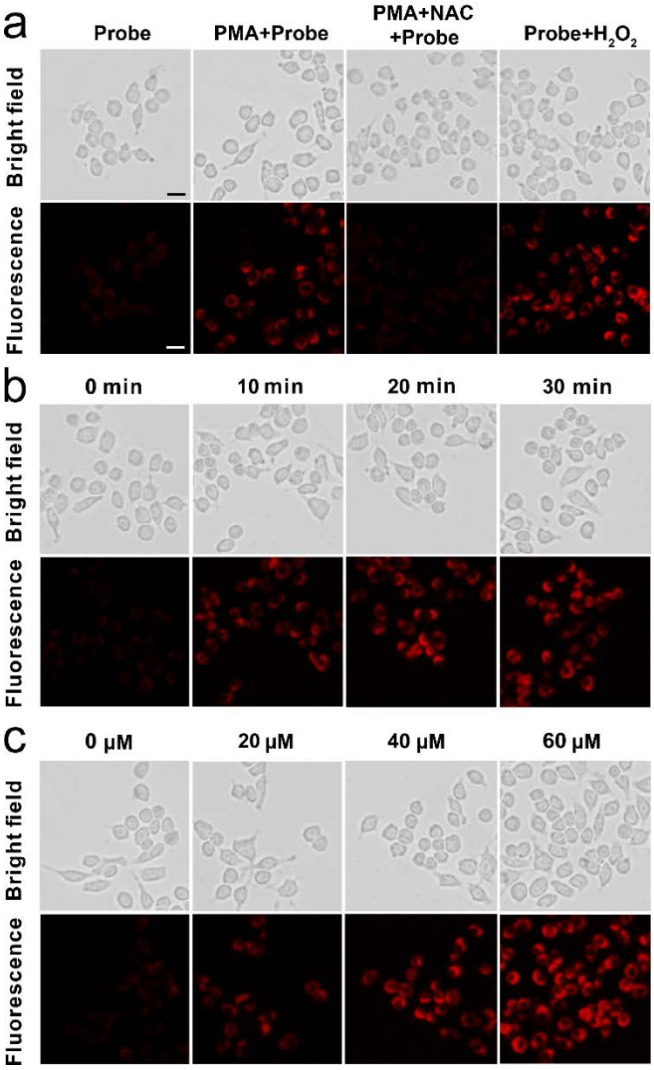

Figure 3 (a) Fluorescence images of RAW264.7 cells incubated with the TA-TPABQ (TPABQ 10 μM) for 30 min; fluorescence images of RAW264.7 pretreated with PMA (1.0 μg/mL, 30 min) and then incubated with the TA-TPABQ (TPABQ 10 μM) for 30 min; fluorescence images of RAW264.7 pretreated with PMA (1.0 μg/mL, 30 min) and followed with treatment of NAC (2 mM, 1 h) and incubated with the TA-TPABQ (TPABQ 10 μM) for 30 min afterwards; fluorescence images of RAW264.7 incubated with the TA-TPABQ (TPABQ 10 μM) for 30 min and then treated with H_2O_2 (60 μM, 30 min). (b) Fluorescence images of RAW264.7 cells incubated with the TA-TPABQ (TPABQ 10 μM) for 30 min, and then treated with H_2O_2 (60 μM) for different time (0-30 min). (c) Fluorescence images of RAW264.7 cells incubated with the TA-TPABQ (TPABQ 10 μM) for 30 min, and then incubated with different concentrations of H_2O_2 (0-60 μM) for 30 min. Scale bar: 20 μm.

Next, we further investigated the response time of the nanoprobe TA-TPABQ towards H_2O_2 in these three living cell lines by incubating the cells with H_2O_2 for different time range (0-30 min). As displayed in Figure 3b, Figure S21b and Figure S22b, the

fluorescence signals enhanced gradually along with the extended incubation time. The flow cytometry experiments were also conducted to assess the nanoprobe's response time toward H_2O_2. As shown in Figure S23a, Figure S23c and Figure S23e, with the prolonged incubation time, the intracellular fluorescence became stronger gradually, indicating that TA-TPABQ was activated in these three cell lines, which were consistent with the above fluorescence imaging results.

After that, the response of the nanoprobe TA-TPABQ towards different concentrations of H_2O_2 (0-60 μM) in these three living cell lines were investigated as well. As shown in Figure 3c, Figure S21c and Figure S22c, the fluorescence signals increased when higher concentrations of H_2O_2 were added into the culture medium of these three cell lines. The flow cytometry analysis with different H_2O_2 concentrations (0-60 μM) are shown in Figure S23b, Figure S23d and Figure S23f, with more exogenous H_2O_2 added, intracellular fluorescence signals became stronger. The results of the flow cytometry analysis were consistent with the fluorescence imaging results. The experimental results indicate that the nanoprobe TA-TPABQ is able to detect the endogenous and exogenous H_2O_2 effectively.

In vivo fluorescence imaging of overexpressed H_2O_2 in mouse models

To evaluate the applicability of the nanoprobe TA-TPABQ in H_2O_2 detection *in vivo*, the biosafety of the TA-TPABQ was investigated. The ICR mice were divided into two groups randomly. For one group, the mice were intravenously (*i.v.*) injected with the TA-TPABQ (2.8 mg nanoprobe/kg body weight) via the tail vein as the probe-treated group. For another group, the mice were injected with the same volume of saline as the control group. The experiments including the mice body weight tracking, hematoxylin and eosin (H&E) staining of main organs' sections (such as the heart, liver, spleen, lung and kidney) were performed. As shown in Figure S24, no abnormal changes in mice body weight in both groups were found. As displayed in Figure S25, histological analysis of the main organs staining with H&E displayed that, there were no obvious damages in the main organs of the probe-treated group, and no obvious differences between the control group and the probe-treated group could be found. The results show that the nanoprobe TA-TPABQ has good biosafety and is suitable to be utilized *in vivo*.

Next, we established the acute abdominal inflammation mouse model to examine the capability of the nanoprobe for imaging the elevated H_2O_2 concentration. The ICR mice were divided into three groups randomly. The first group were injected with the nanoprobe TA-TPABQ into the peritoneal cavity (as the control group); the second group of mice were injected with the stimulator rotenone[56] and followed with the injection of the TA-TPABQ intraperitoneally (as the stimulated group); and the third group of mice were intraperitoneally injected with the rotenone and then successively with NAC and the TA-TPABQ (as the inhibited group). The mice were then submitted to imaging, and the results are shown in Figure 4a. The mouse in control group displayed relatively weak fluorescence intensity in the abdominal region, and the fluorescence intensity increased obviously in the stimulated group, which may be attributed to the enhanced level of endogenous H_2O_2 induced by the stimulator rotenone. By contrast, the fluorescence intensity in the inhibited group weakened because of the inhibitory action of NAC, since NAC is a common reductant to scavenge the oxygen species. The quantified mean fluorescence intensities for the three groups are shown in Figure 4b. The results indicate that the TA-TPABQ is capable of detecting the elevated H_2O_2 in abdominal inflammation.

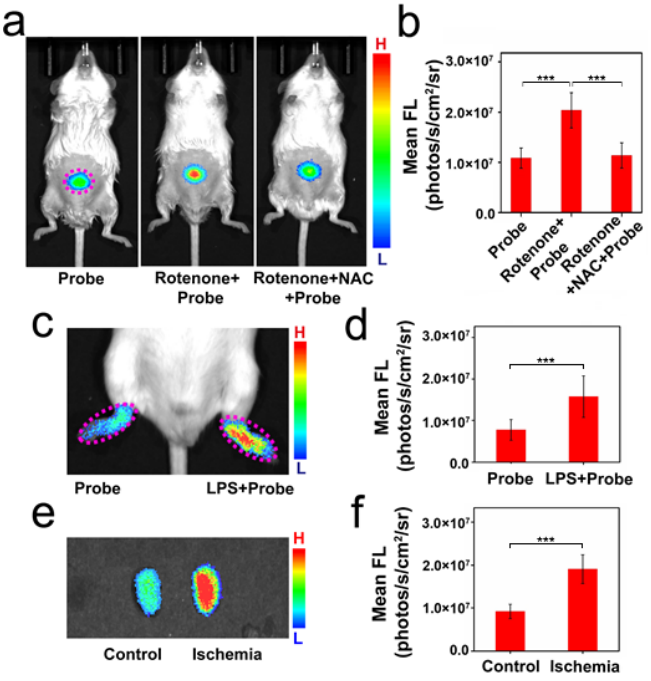

Figure 4 (a) Fluorescence imaging of H_2O_2 in the mouse model with acute abdominal inflammation. The mouse only injected with the nanoprobe TA-TPABQ was used as the control; the mouse pretreated with rotenone for 1 h and followed with the injection of the nanoprobe TA-TPABQ; the mouse successively injected with rotenone, NAC and followedwith the injection of the nanoprobe TA-TPABQ. (b) Mean fluorescence intensities for the region of interest (ROI, in red circle) in the mouse models in (a). (c) Fluorescence imaging of H_2O_2 in the mouse model with acute ankle inflammation. The nanoprobe TA-TPABQ was injected into the left hind ankle; and LPS and the nanoprobe TA-TPABQ were successively injected into the right hind ankle. (d) Mean fluorescence intensities for the ROI (red circles) in mouse model in (c). (e) Fluorescence images of the isolated left kidney (control) and right kidney (ischemic kidney model) of ICR mouse. (f) Mean fluorescence intensities of the isolated left kidney (control) and right kidney (suffered from acute ischemia) in (e). Columns represent mean ± SD. ***p <0.001.

Afterwards the acute ankle inflammation mouse model was established to further evaluate the nanoprobe's capability to image the elevated endogenous H_2O_2 *in vivo*. The ICR mice' right hind ankles were injected with the TA-TPABQ as the control side, while their left hind ankles were successively injected with the lipopolysaccharide (LPS, 2.0 μg/mL in saline) and the TA-TPABQ as the LPS-treated side. The fluorescence images are shown in Figure 4c; the fluorescence intensity in the left ankle was stronger than that in the right ankle (control), since the LPS is a widely used

inflammation inducer, which may leads to the up-regulation of H_2O_2.[57] And the quantified mean fluorescence intensities for the LPS-treated side and the control side are shown in Figure 4d. The results confirm that the nanoprobe TA-TPABQ can be used to image the elevated H_2O_2 concentration in acute inflammation diseases.

To further explore the nanoprobe's capability to be applied in other disease models, the acute ischemic kidney injury mouse model was established. Ischemia of organs usually occurs with the insufficient supply of blood to the organs, which can disrupt the normal functions of organs.[58] Excessive production of ROS may be accompanied with the aberrant immune responses in the ischemic organs.[59] In this experiment, the mice were anesthetized, and the ischemia in the right kidneys was induced through the vessel ligation (as the ischemia side), while the left kidneys without vessel ligation acted as the control side. Then the nanoprobe TA-TPABQ was injected via tail vein after the removal of ligation, and then both the kidneys were harvested from the mice. As displayed in Figure 4e, the fluorescence signal of the right kidney increased significantly, while for the control side of the left kidney, the fluorescence signal was relatively lower. The corresponding quantitative fluorescence data are displayed in Figure 4f. The above experimental results demonstrate that the nanoprobe TA-TPABQ can detect the elevated H_2O_2 in acute inflammations and ischemic kidney injury *in vivo*.

Conclusions

The near-infrared fluorescent nanoprobe TA-TPABQ was developed successfully, which was prepared through the boronate ester bonds (dynamic covalent bonding) between the compound TPABQ and tannic acid as well as the aggregation induced by hydrophobic interaction. Upon the nanoprobe's reaction with H_2O_2 the fluorophore TPAQ-OH is released, which shows an obvious turn-on fluorescence signal with AIE feature and a large Stokes shift of 198 nm. Moreover, the nanoprobe has been successfully utilized to image the endogenous and exogenous H_2O_2 in three cell lines (RAW264.7, HepG2 and HeLa). Furthermore, this nanoprobe has been applied to detect the over-expressed H_2O_2 in the acute abdominal inflammation mouse model, the acute ankle inflammation mouse model and the ischemic kidney injury mouse model. Hence, this nanoprobe holds promise for serving as an effective tool for detecting H_2O_2 overexpression in related diseases.)

Experimental

Preparation process and characterization of TA-TPABQ

Detailed synthetic routes were illustrated in the Supporting Information, as shown in Scheme S1 and Scheme S2, and the corresponding characterizations of intermediate products and the final nanoprobe TA-TPABQ were provided in Figure S1-Figure S9.

General spectra analysis procedure

The spectra analysis procedures were according to the previous literatures[60] with slight modifications. In detail, the fluorescence spectra were recorded at the excitation of 580 nm and the emission range from 650 nm to 900 nm. The stock solution of the nanoprobe TA-TPABQ was prepared by dispersing it into the PBS (10 mM, pH 7.4). For response performance test, the test solution was prepared with addition of the stock solution of the nanoprobe TA-TPABQ, different concentrations of H_2O_2 was added with final 3 mL volume in total. For selectivity experiments, the nanoprobe solutions were incubated with H_2O_2 or other analytes, such as the reactive sulfur species, amino acids, cations and anions for 30 min (in PBS, 10 mM pH 7.4).

Cell imaging experiment

For cell imaging experiments, the procedures were proceeded according to the previous studies[61,62] with necessary modifications herein. In detail, three cell lines such as HeLa cell line (human cervical cancer cell line), HepG2 cell line (human hepatoma cell line) and RAW264.7 cell line (mouse macrophage cell line) were seeded inside 35 mm glass culture dishes in the corresponding complete medium for adherence. After incubation for over 12 h, the culture dishes were washed with PBS, then filled with the corresponding fresh medium. In one experiment, one group of cells in the 6-well culture dishes were cultured with the nanoprobe TA-TPABQ (TPABQ 10 μM); another group was pre-treated with phorbol myristate acetate (PMA, 1.0 μg/mL, 30 min), then incubated with the nanoprobe TA-TPABQ (TPABQ 10 μM); the third group was pre-treated with PMA, then treated with N-acetylcysteine (NAC), and then with the nanoprobe TA-TPABQ (TPABQ 10 μM); the last group was pre-treated with the nanoprobe TA-TPABQ (TPABQ 10 μM) and incubated with the exogenous H_2O_2 (60 μM) for 30 min. In another experiment, the three cell lines were cultured with the nanoprobe TA-TPABQ, and followed with incubation with H_2O_2 (60 μM) for different culture time (0 min, 10 min, 20 min, 30 min). In another experiment, three cell lines were incubated with the nanoprobe TA-TPABQ (TPABQ 10 μM) for 30 min, subsequently incubated with different concentrations of H_2O_2 (0 μM, 20 μM, 40 μM and 60 μM) for 30 min. All the culture dishes were placed in the humidified incubator Forma™ Steri-Cult™ (ThermoFisher, USA) at 37 °C, containing 5% CO_2. Prior to the cell imaging experiment, cells were rinsed with PBS three times to remove the culture medium, then subjected to fluorescence microscope imaging. An Olympus IX71 inverted fluorescence microscope with DP72 color CCD was employed for fluorescence imaging.

Fluorescent imaging in animal models

The animal experiments were performed in the Laboratory Animal Center of South China Agricultural University (SCAU), and the animals were maintained under Specific Pathogen-Free (SPF) conditions. All the experimental protocols have been approved and conducted according to the guidelines and regulations of Animal Ethics Committee of SCAU for the care and use of laboratory animals, and the experiments were conducted in compliance with the regulations on the management of laboratory animals of China. Herein, ICR mice (5-6 weeks old) for in vivo imaging were provided by Guangdong Medical Laboratory Animal Center (GDMLAC).

The acute abdominal inflammation model experiments were conducted as follows: In detail, the mice were fasted for 12 h. The mice were divided into the control group, the stimulated group and the inhibited group. Then the mice were anesthetized with 2.0% isoflurane by inhalation during the operation procedure. The mice

in the control group were given with an injection of TA-TPABQ (2.8 mg probe/kg body weight) into the peritoneal cavity. The mice in the stimulated group was pre-treated with the rotentone (2 mM) into the peritoneal cavity, followed with intraperitoneal (*i.p.*) injection of the nanoprobe TA-TPABQ (2.8 mg probe/kg body weight) in the same region 2 h later. The mice in the inhibited group was successively treated with the rotentone (2 mM) for 1 h, then followed with *i.p.* injection of NAC (20 mM) for 1 h, then the nanoprobe TA-TPABQ (2.8 mg probe/kg body weight) was *i.p.* injected into the same region. 15 min after the probe injection, fluorescence imaging was then acquired by using Ami small animal-imaging system (SI Imaging Company), with excitation filter 560 nm and emission filter of 730 nm.

The ankle inflammation mouse model experiment was conducted as follows. Prior to the experiment, the ICR mice were anesthetized with 2.0% isoflurane by inhalation. In detail, the left hind ankles of ICR mice were injected with LPS (2.0 μg/mL in saline) to induce the acute inflammation. Then the nanoprobe TA-TPABQ (2.0 mg probe/kg body weight) was injected into the same region of the ankles with inflammation after the LPS treatment for 24 h. And the right hind ankles were acted as the control side without any treatment with the stimulators. 15 min after the probe injection, fluorescent images were taken through an Ami small animal-imaging system (SI imaging Company) with an excitation 560 nm filter and an emission 730 nm filter.

The acute ischemic kidney injury mouse model experiment was conducted as follows: Before the imaging procedure, the ICR mice were fasted for 12 h. The mice were anesthetized with 2.0% isoflurane inhalation and the simple laparotomy operation was performed to induce the inflammation of renal ischemia. In detail, the abdominal cavity was exposed, and the corresponding right renal artery was clamped, the acute renal ischemia was induced. In the control group, the left kidney was exposed without any operation. After one hour, the ligation of the right kidney was removed. Then the mice were injected with the nanoprobe TA-TPABQ (2.8 mg probe/kg body weight) via the tail vein. At 15 min after probe injection, the mice was sacrificed under excessive CO_2 atmosphere, the kidneys were isolated and allowed for fluorescence imaging process by using an Ami small animal-imaging system (SI imaging Company) with 560 nm excitation filter and 730 nm emission filter.

Supporting Information

The supporting information for this article is available on the WWW under https://doi.org/10.1002/cjoc.2018xxxxx.

Acknowledgement

This work was supported by NSFC (51673066, 21875069 and 21574044), the Natural Science Foundation of Guangdong Province (2016A030312002) and the Fund of Guangdong Provincial Key Laboratory of Luminescence from Molecular Aggregates (2019B030301003).

References

[1] Rhee, S. G. H_2O_2, a necessary evil for cell signaling. *Science* **2006**, *312*, 1882-1883.

[2] Veal, E. A.; Day, A. M.; Morgan, B. A. Hydrogen peroxide sensing and signaling. *Cell* **2007**, *26*, 1-14.

[3] Du, F. K.; Min, Y. H.; Zeng, F.; Yu, C. M.; Wu, S. A targeted and FRET-based ratiometric fluorescent nanoprobe for imaging mitochondrial hydrogen peroxide in living cells. *Small* **2014**, *10*, 964-972.

[4] Battin, E. E.; Brumaghim, J. L. Antioxidant activity of sulfur and selenium: a review of reactive oxygen species scavenging, glutathione peroxidase, and metal-binding antioxidant mechanisms. *Cell Biochem. Biophys.* **2009**, *55*, 1-23.

[5] McBean, G. J.; Aslan, M.; Griffiths, H. R.; Torrao, R. C. Thiol redox homeostasis in neurodegenerative disease. *Redox Biol.* **2015**, *5*, 186-194.

[6] Circu, M. L.; Aw, T. Y. Reactive oxygen species, cellular redox systems, and apoptosis. *Free Radical Biol. Med.* **2010**, *48*, 749-762.

[7] Lopez-Lazaro, M. Dual role of hydrogen peroxide in cancer: possible relevance to cancer chemoprevention and therapy. *Cancer Lett.* **2007**, *252*, 1-8.

[8] Wu, Y. L.; Wang, J.; Zeng, F.; Huang, S.; Huang, J.; Xie, H.; Yu, C.; and Wu, S. Pyrene derivative emitting red or near-Infrared light with monomer/excimer conversion and its application to ratiometric detection of hypochlorite. ACS Appl. Mater. Interfaces **2016**, *8*, 1511-1519.

[9] Xie, X. L.; Yang, X.; Wu, T. H.; Li, Y.; Li, M. M.; Tan, Q.; Wang, X.; Tang, B. Rational design of an α-ketoamide-based near-infrared fluorescent probe specific for hydrogen peroxide in living systems. *Anal. Chem.* **2016**, *88*, 8019-8025.

[10] Narayanaswamy, N.; Narra, S.; Nair, R. R.; Saini, D. K.; Kondaiah, P.; Govindaraju, T. Stimuli-responsive colorimetric and NIR fluorescence combination probe for selective reporting of cellular hydrogen peroxide. *Chem. Sci.* **2016**, *7*, 2832-2841 .

[11] Dong, S. Y.; Su, M. H.; Nie, L. H.; Ma, H. M. A novel fluorescent reagent for analysis of hydrogen peroxide. *Chin. J. Chem.* **2003**, *21*, 189-191.

[12] Li, H. D.; Yao, Q. C.; Fan, J. L.; Wang, J. J.; Peng, X. J. A two-photon NIR-to-NIR fluorescent probe for imaging hydrogen peroxide in living cells. *Biosens. Bioelectron.* **2017**, *94*, 536-543.

[13] Qi, Y.; Huang, Y.; Li, B.; Zeng, F.; Wu, S. Real-time monitoring of endogenous cysteine levels in vivo by near-Infrared turn-on fluorescent probe with large stokes shift, *Anal. Chem.* **2018**, *90*, 1014-1020.

[14] Yu, F. B.; Han, X. Y.; Chen, L. X. Fluorescent probes for hydrogen sulfide detection and bioimaging. *Chem.Commun.* **2014**, *50*, 12234-12249

[15] Wu, Y.; Huang, S.; Wang, J.; Sun, L.; Zeng, F.; Wu, S. Activatable probes for diagnosing and positioning liver injury and metastatic tumors by multispectral optoacoustic tomography. *Nat. Commun.* **2018**, *9*, 3983.

[16] Sun, L.; Wu, Y.; Chen, J.; Zhong, J.; Zeng, F.; Wu, S. A turn-on optoacoustic probe for imaging metformin-induced upregulation of hepatic hydrogen sulfide and subsequent liver injury. *Theranostics*. **2019**, *9*, 77-89.

[17] Wen, Y.; Huo, F. J.; Yin, C. X. Organelle targetable fluorescent probes for hydrogen peroxide. *Chin. Chem. Lett.* **2019**, *30*, 1834-1842.

[18] Chen, C.; Ou, H. L.; Liu, R. H.; Ding, D. Regulating the photophysical property of organic/polymer optical agents for promoted cancer phototheranostics. *Adv. Mater.* **2019**, *31*, 1806331.

[19] Zhang, Y. T.; Yan, C. X.; Wang, C.; Guo, Z. Q.; Liu, X. G.; Zhu, W. H. A Sequential dual-lock strategy for photoactivatable chemiluminescent

probes enabling bright duplex optical imaging. *Angew. Chem. Int. Ed.* **2020**, 10.1002/anie.202000165.

[20] Mao, W. L.; Zhu, M. M.; Yan, C. X.; Ma, Y. Y.; Guo, Z. Q.; Zhu, W. H. Rational design of ratiometric near-infrared aza-BODIPY-based fluorescent probe for in vivo imaging of endogenous hydrogen peroxide. *ACS Appl. Bio Mater.* **2020**, *3*, 45-52.

[21] Guo, H. L.; Chen, G.; Gao, M.; Wang, R.; Liu, Y. X.; Yu, F. B. Imaging of endogenous hydrogen peroxide during the process of cell mitosis and mouse brain development with a near-infrared ratiometric fluorescent probe. *Anal. Chem.* **2019**, *91*, 1203-1210.

[22] Lippert, A. R.; Van de Bittner, G. C.; Chang, C. J. Boronate oxidation as a bioorthogonal reaction approach for studying the chemistry of hydrogen peroxide in living systems. *Acc. Chem. Res.* **2011**, *44*, 793-804.

[23] Chen, X. Q.; Tian, X. Z.; Shin, I.; Yoon, J. Y. Fluorescent and luminescent probes for detection of reactive oxygen and nitrogen species. *Chem. Soc. Rev.* **2011**, *40*, 4783-4804.

[24] Ouyang, J.; Sun, L. H.; Zeng, Z.; Zeng, C.; Zeng, F.; Wu, S. Z. Nanoaggregate probe for breast cancer metastasis through multispectral optoacoustic tomography and aggregation-induced NIR-I/II fluorescence imaging. *Angew. Chem. Int. Ed.* **2019**, doi: 10.1002/anie.201913149.

[25] Yan, L. L.; Zhang, Y.; Xu, B.; Tian, W. J. Fluorescent nanoparticles based on AIE fluorogens for bioimaging. *Nanoscale*, **2016**, *8*, 2471-2487.

[26] Ding, D.; Li, K.; Liu, B.; Tang, B. Z. Bioprobes based on AIE fluorogens. *Acc. Chem. Res.* **2013**, *46*, 2441-2453.

[27] Zhang, S. B.; Guo, W. S.; Wei, J.; Li, C.; Liang, X. J.; Yin, M. Z. Terrylenediimide-based intrinsic theranostic nanomedicines with high photothermal conversion efficiency for photoacoustic imaging-guided cancer therapy. *ACS Nano* **2017**, *11*, 3797-3805.

[28] Zong, L. Y.; Xie, Y. J.; Wang, C. J.; Li, R.; Li, Q. Q.; Li, Z. From ACQ to AIE: the suppression of the strong π–π interaction of naphthalene diimide derivatives through the adjustment of their flexible chains. *Chem. Commun.* **2016**, *52*, 11496-11499.

[29] Yu, C.; Li, X.; Zeng, F.; Zheng, F.; Wu, S. Carbon-dot-based ratiometric fluorescent sensor for detecting hydrogen sulfide in aqueous media and inside live cells, *Chem. Commun.* **2013**, *49*, 403-405.

[30] Hang, Y. D.; Wang, J.; Jiang, T.; Lu, N. N.; Hua, J. L. Diketopyrrolopyrrole-based ratiometric/turn-on fluorescent chemosensors for citrate detection in the near-Infrared region by an aggregation-induced emission mechanism. *Anal. Chem.* **2016**, *88*, 1696-1703.

[31] Li, Q. Q.; Li, Z. The strong light-emission materials in the aggregated state: what happens from a single molecule to the collective group. *Adv. Sci.* **2017**, *4*, 1600484 (1-15).

[32] Chen, S. J.; Wang, H.; Hong, Y. N.; Tang, B. Z. Fabrication of fluorescent nanoparticles based on AIE luminogens (AIE dots) and their applications in bioimaging. *Mater. Horiz.* **2016**, *3*, 283-293.

[33] Shao, A. D.; Xie, Y. S.; Zhu, S. J.; Guo, Z. Q.; Zhu, S. Q.; Guo, J.; Shi, P.; James, T. D.; Tian, H.; Zhu, W. H. Far-red and near-IR AIE-active fluorescent organic nanoprobes with enhanced tumor‐targeting efficacy: shape-specific effects. *Angew. Chem. Int. Ed.* **2015**, *54*, 7275-7280.

[34] Tang, X. J.; Zhang, L. H.; Hu, R. R.; Tang, B. Z. Multicomponent tandem polymerization of aromatic alkynes, carbonyl chloride, and fischer's base toward poly(diene merocyanine)s. *Chin. J. Chem.* **2019**, *37,* 1264-1270.

[35] Chu, Y. C.; Xie, Z. F.; Zhuang, D. J.; Yue, Y. S.; Yue, Y. H.; Shi, W.; Feng, S. An intramolecular charge transfer and aggregation induced emission enhancement fluorescent probe based on 2-Phenyl-1,2,3-triazole for highly selective and sensitive detection of homocysteine and its application in living cells. *Chin. J. Chem.* **2019**, *37*, 1216-1222.

[36] Yuan, Q. M.; Cheng, Y.; Lou X. D.; Xia, F. Rational fabrication and biomedical application of biomolecule-conjugated AIEgens through click reaction. *Chin. J. Chem.* **2019**, *37*, 1072-1082.

[37] Ni, X.; Zhang, X. Y.; Duan, X. C.; Zheng, H. L.; Xue, X. S.; Ding, D. Near-infrared afterglow luminescent aggregation-induced emission dots with ultrahigh tumor-to-liver signal ratio for promoted image-guided cancer surgery. *Nano Lett.* **2019**, *19*, 318-330.

[38] Chen, C.; Ni, X.; Jia, S. R.; Liang, Y.; Wu, X. L.; Kong, D. L.; Ding, D. Massively evoking immunogenic cell death by focused mitochondrial oxidative stress using an AIE luminogen with a twisted molecular structure. *Adv. Mater.* **2019**, *31*, 1904914.

[39] Song, Z. G.; Mao, D.; Sung, S. H. P.; Kwok, R. T. K.; Lam, J. W. Y.; Kong, D. L.; Ding, D.; Tang, B. Z. Activatable fluorescent nanoprobe with aggregation-induced emission characteristics for selective in vivo imaging of elevated peroxynitrite generation. *Adv. Mater.* **2016**, *28*, 7249-7256.

[40] Zhang, W.; Liu, W.; Li, P.; Huang, F.; Wang, H.; Tang, B. Rapid-response fluorescent probe for hydrogen peroxide in living cells based on increased polarity of C–B bonds. *Anal. Chem.* **2015**, *87*, 9825-9828.

[41] Hu, F.; Huang, Y. Y.; Zhang, G. X.; Zhao, R.; Zhang, D. Q. A highly selective fluorescence turn-on detection of hydrogen peroxide and d-glucose based on the aggregation/deaggregation of a modified tetraphenylethylene. *Tetrahedron Lett.* **2014**, *55*, 1471-1474.

[42] Liu, J.; Zhang, C. H.; Dong, J.; Zhu, J.; Shen, C. Y.; Yang, G. Q.; Zhang, X. M. Nanogel-loading a triarylboron-based AIE fluorophore to achieve ratiometric sensing for hydrogen peroxide and sequential response for pH. *New J. Chem.* **2017**, *41*, 4733-4737.

[43] Liu, G. J.; Long, Z.; Lv, H. J.; Li, C. Y.; Xing, G. W. A dialdehyde–diboronate-functionalized AIE luminogen: design, synthesis and application in the detection of hydrogen peroxide. *Chem. Commun.* **2016**, *52*, 10233-10236.

[44] Liao, Y. X.; Li, K.; Wu, M. Y.; Wu, T.; Yu, X. Q. A selenium-contained aggregation-induced "turn-on" fluorescent probe for hydrogen peroxide. *Org. Biomol. Chem.* **2014**, *12*, 3004-3008.

[45] Su, J.; Chen, F.; Cryns, V. L.; Messersmith, P. B. Catechol polymers for pH-responsive, targeted drug delivery to cancer cells. *J. Am. Chem. Soc.* **2011**, *133*, 11850-11853.

[46] Hu, X.; Chai, Z.; Lu, L.; Ruan, H.; Wang, R.; Zhan, C.; Xie, C.; Pan, J.; Liu, M.; Wang, H.; Lu, W. Bortezomib dendrimer prodrug-based nanoparticle system. *Adv. Funct. Mater.* **2019**, *29*, 1807941.

[47] Ye, Q.; Zhou, F.; Liu, W. Bioinspired catecholic chemistry for surface modification. *Chem. Soc. Rev.* **2011**, *40*, 4244-4258.

[48] Karton-Lifshin, N.; Segal, E.; Omer, L.; Portnoy, M.; Satchi-Fainaro, R.; Shabat, D. A unique paradigm for a Turn-ON near-infrared cyanine-based probe: noninvasive intravital optical imaging of hydrogen peroxide. *J. Am. Chem. Soc.* **2011**, *133*, 10960-10965.

[49] Dickinson, B. C.; Huynh, C.; Chang, C. J. A palette of fluorescent probes with varying emission colors for imaging hydrogen peroxide signaling in living cells. *J. Am. Chem. Soc.* **2010**, *132*, 5906-5915.

[50] Yuan, L.; Lin, W.; Xie, Y.; Chen, B.; Zhu, S. Single fluorescent probe

responds to H_2O_2, NO, and H_2O_2/NO with three different sets of fluorescence signals. *J. Am. Chem. Soc.* **2012**, *134*, 1305-1315.

[51] Wu, Y. L.; Chen, J. J.; Sun, L. H.; Zeng, F.; Wu, S. Z. Diagnosing drug-induced liver injury by multispectral optoacoustic tomography and fluorescence imaging using a leucine-aminopeptidase-activated probe. *Adv. Funct. Mater.* **2019**, *29*, 1807960.

[52] Wang, D.; Su, H. F.; Kwok, R. T. K.; Hu, X. L.; Zou, H.; Luo, Q. X.; Lee, M. M.; Xu, S. W. H.; Lam, J. W. Y.; Tang, B. Z. Rational design of a water-soluble NIR AIEgen, and its application in ultrafast wash-free cellular imaging and photodynamic cancer cell ablation. *Chem. Sci.* **2018**, *9*, 3685-3693.

[53] Chang, J. F.; Li, H. Y.; Hou, T.; Duan, W. N.; Li, F. Paper-based fluorescent sensor via aggregation induced emission fluorogen for facile and sensitive visual detection of hydrogen peroxide and glucose. *Biosens. Bioelectron.* **2018**, *104*, 152-157.

[54] Dickinson, B. C.; Huynh, C.; Chang, C. J. A palette of fluorescent probes with varying emission colors for imaging hydrogen peroxide signaling in living cells. *J. Am. Chem. Soc.* **2010**, *132*, 5906-5915.

[55] Ishikawa, K.; Takenaga, K.; Akimoto, M.; Koshikawa, N.; Yamaguchi, A.; Imanishi, H.; Nakada, K.; Honma, Y.; Hayashi, J. I. ROS-generating mitochondrial DNA mutations can regulate tumor cell metastasis. *Science* **2008**, *320*, 661-664.

[56] Mansouri, A.; Muller, F. L.; Liu, Y.; Ng, R.; Faulkner, J.; Hamilton, M.; Richardson, A.; Huang, T. T.; Epstein, C. J.; Van Remmen, H. Alterations in mitochondrial function, hydrogen peroxide release and oxidative damage in mouse hind-limb skeletal muscle during aging. *Mech. Ageing Dev.* **2006**, *127*, 298-306.

[57] Zhao, W. J.; Li, Y. H.; Yang, S.; Chen, Y.; Zheng, J.; Liu, C. H.; Qing, Z. H.; Li, J. S.; Yang, R. H. Target-activated modulation of dual-color and two-photon fluorescence of graphene quantum dots for in vivo imaging of hydrogen peroxide. *Anal. Chem.* **2016**, *88*, 4833-4840.

[58] Zhai, B. P.; Hu, W.; Hao, R. L.; Ni, W. J.; Liu, Z. H. Development of a ratiometric two-photon fluorescent probe for imaging of hydrogen peroxide in ischemic brain injury. *Analyst* **2019**, *144*, 5965-5970.

[59] Hung, L. M.; Su, M. J.; Chu, W. K.; Chiao, C. W.; Chan, W. F.; Chen, J. K. The protective effect of resveratrols on ischaemia-reperfusion injuries of rat hearts is correlated with antioxidant efficacy. *Br. J. Pharmacol.* **2002**, *135*, 1627-1633.

[60] Song, Z. G.; Kwok, R. T. K.; Ding, D.; Nie, H.; Lam, J. W. Y.; Liu, B.; Tang, B. Z. An AIE-active fluorescence turn-on bioprobe mediated by hydrogen-bonding interaction for highly sensitive detection of hydrogen peroxide and glucose. *Chem. Commun.* **2016**, *52*, 10076-10079.

[61] Ren, M. G.; Deng, B. B.; Zhou, K.; Kong, X. Q.; Wang, J. Y.; Lin, W. Y. Single fluorescent probe for dual-imaging viscosity and H_2O_2 in mitochondria with different fluorescence signals in living cells. *Anal. Chem.* **2017**, *89*, 552-555.

[62] Zeng, Q.; Zhang, R. J.; Zhang, T.; Xing, D. H_2O_2-responsive biodegradable nanomedicine for cancer-selective dual-modal imaging guided precise photodynamic therapy. *Biomaterials* **2019**, *207*, 39-48.

(The following will be filled in by the editorial staff)
Manuscript received: XXXX, 2019
Manuscript revised: XXXX, 2019
Manuscript accepted: XXXX, 2019
Accepted manuscript online: XXXX, 2019
Version of record online: XXXX, 2019

Entry for the Table of Contents

Page No.

Near-infrared fluorescent nanoprobe for detecting hydrogen peroxide in inflammation and ischemic kidney injury

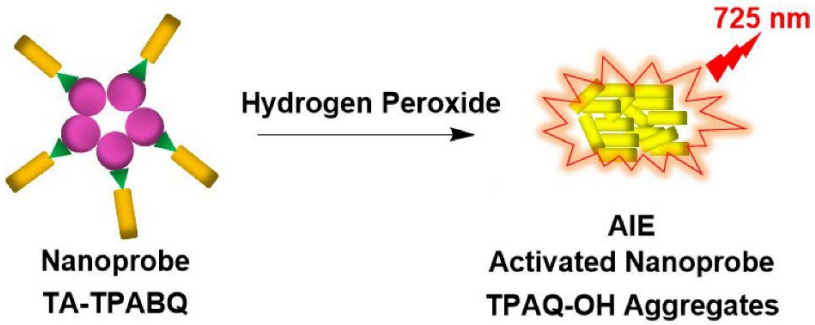

Yingfeng Xu, Lihe Sun, Fang Zeng,*[,a] Shuizhu Wu,*[,a]

A nanoprobe with activated AIE feature was developed for monitoring the overexpression of hydrogen peroxide in inflammation and ischemic kidney injury.

[a] *State Key Laboratory of Luminescent Materials & Devices, Guangdong Provincial Key Laboratory of Luminescence from Molecular Aggregates, College of Materials Science & Engineering, South China University of Technology, Guangzhou 510640, China*
E-mail: mcfzeng@scut.edu.cn; shzhwu@scut.edu.cn.

Chin. J. Chem. **2018**, template© 2018 SIOC, CAS, Shanghai, & WILEY-VCH Verlag GmbH & Co. KGaA, Weinheim